

Characterization of sol-gel derived yttrium-doped n-ZnO/p-Si heterostructure

N. KUMAR¹, R. KAUR², R. M. MEHRA^{3*}

¹Department of Electronics, Sri Venkateswara College, University of Delhi, New Delhi 110021, India

²Department of Physics and Electronics, Deen Dayal Upadhyay College,
University of Delhi, New Delhi 110015, India

³Department of Electronic Science, University of Delhi South Campus, New Delhi 110021, India

The paper reports the experimental and theoretical analysis of current–voltage characteristics of n-ZnO/p-Si (100) heterostructures. Yttrium-doped ZnO films were deposited on p-Si by the sol-gel process using the spin coating technique. Their structural and electrical properties were studied as a function of annealing temperature. The experimental data were analysed by modifying the current voltage relation predicted by Perlman and Feucht. An estimate of the defect density at the ZnO/Si interface was made using Mott–Schottky (C^{-2} – U) plots.

Key words: *sol-gel; yttrium-doped ZnO; heterostructure; I–U characteristics; C–U characteristics*

1. Introduction

It is well recognized that a reliable and mass-produceable blue-ultraviolet semiconductor diode laser will have a major importance in information storage, display, photochemistry, and other areas of technology. GaN-based lasers and LEDs are already achieving commercial realization and undergoing improvements in lifetime and synthesis techniques. ZnO has been used for decades in powder form for phosphors and in polycrystalline form for varistors. ZnO has a direct band gap of 3.3 eV at room temperature, comparable to that of GaN. It is refractory, with a melting point of 1975 °C compared to 1100 °C for ZnSe, leading us to expect that it will be more robust with regard to defect generation under electronic and thermal stress. In contrast to GaN, large single crystals of ZnO can easily be grown. The exciton binding energy in ZnO is 60 meV, three times larger than that of ZnSe or GaN, and more than twice as

* Corresponding author, e-mail: rammehra2003@yahoo.com

large as kT at room temperature (RT) [1]. This means that the recombination and luminescence properties of ZnO should retain exciton characteristics at and above RT, including the substantial enhancement of oscillator strength. ZnO thin films can be prepared by a wide variety of techniques, including sputtering [2], reactive evaporation [3], chemical vapour deposition [4], spray pyrolysis [5], and the sol-gel [6] process. In particular, the sol-gel method has advantages over the other processes, because of its simplicity and low equipment cost. With regards to the transparent and conducting window layer for optoelectronic devices, ZnO has an additional advantage over ITO – it is able to tolerate reducing chemical environments. For instance, ZnO films are more stable than ITO-based films in the presence of hydrogen plasma. They can match, if not exceed, optical and electrical properties of ITO. Furthermore, the components of ITO, namely In and Sn, are limited in supply and are more expensive than zinc.

A renewed interest in the luminescence and electrical properties of ZnO/Si heterostructures has also emerged. There have been reports on undoped n-ZnO/p-Si heterostructures fabricated by magnetron sputtering, chemical vapour deposition and spray pyrolysis. Jeong et al. [7] and Lee et al. [8] have reported the fabrication of an undoped n-ZnO/p-Si photodiode by sputter deposition. They have also reported that the fabricated photodiode exhibits good photoelectric performance when ZnO is deposited at 480 °C. It has also been concluded that the photodiode exhibits an induced photocurrent proportional to the reverse bias for UV illumination and saturation at moderate bias for visible illumination. Park et al. [9] have reported that there is an effective reduction in the dark leakage current after implanting Si^+ ions into the device structure of insulating ZnO and semiconducting n-ZnO overlayers on p-Si. Thin film ZnO/InP and ZnO/Si heterojunctions obtained by thermal decomposition of Zn acetylacetonate have been investigated by Purica et al. [10] for optoelectronic device applications. Baik et al. [11] have studied Al-doped ZnO/n-Si junction solar cells prepared by spin coating.

In the present work, n-type ZnO films, pure and yttrium-doped, have been grown on p-silicon substrates by spin coating, using zinc acetate and ethanol as the precursors and DEA as the stabilizer. The effects of yttrium doping on the structural, electrical and optical properties of the films are reported.

The I – U characteristics of n-ZnO/p-Si heterostructures have been studied as a function of annealing temperature, and analysed by taking into account the diffusion and generation recombination current [12]. An estimate of the defect density at the ZnO-Si interface has been made using capacitance-voltage (C – U) measurements [13].

2. Experimental

The precursor solution of ZnO (0.2 M) was prepared from zinc acetate ($\text{Zn}(\text{CH}_3\text{CO}_2)_2 \cdot 2\text{H}_2\text{O}$, purity 99.5%) dissolved in anhydrous ethanol. Yttrium nitrate hexahydrate ($\text{Y}_2\text{NO}_3 \cdot 6\text{H}_2\text{O}$) was used as the dopant (3 wt. %). The mixture so ob-

tained was stirred with a magnetic stirrer for about 4 h at room temperature, after which it remained milky. An equimolar amount of diethanolamine (DEA) was added to the solution drop by drop which eliminated the obtained turbidity and precipitates completely. The resultant solution was very clear, transparent, and homogenous. The solution was left to age for 48 h to obtain optimum viscosity before film deposition. The corning glass (7059) substrates, after being cleaned with acetone and methanol in an ultrasonic bath for 20 minutes, were rinsed with deionised water for 5 min and dried in a nitrogen atmosphere. The Si ($2\text{--}4\ \Omega\text{cm}$ resistivity) samples were cleaned in trichloroethylene, acetone and isopropyl acetate consecutively for 10 min in an ultrasonic bath. The substrates were rinsed in overflowing deionised water for 10 min and treated with a 2% HF solution in order to remove the native oxide, then washed with deionised water for 20 minutes, and dried with dry nitrogen gas. The deposition of yttrium-doped zinc oxide (YZO) film was carried at room temperature with a spinning speed of 2700 rpm for 20 sec. The films were left in air for 10 min to hydrolyse (by esterification) and then dried in air at $250\ ^\circ\text{C}$ in order to gel. The process was repeated 12 to 15 times to obtain the film thickness of ca. 250 nm. The films were annealed in air in the temperature range $300\text{--}600\ ^\circ\text{C}$ for an hour. The YZO films so developed exhibit n-type conductivity [14].

The structural properties of the films were investigated with an X-ray diffractometer. The thickness of the ZnO layer was measured with a Dektak^{3-ST} surface profilometer. The $I\text{--}U$ characteristics of these heterostructures were recorded using a Keithley Source Meter (2400) and $C\text{--}U$ measurements were carried on a Biorad $C\text{--}U$ meter (DL 4600) using a voltage source (4140 V) and a Boonton capacitance meter. Optical transmittance measurements were carried out in the wavelength range $200\text{--}800\ \text{nm}$ using a double beam spectrophotometer (Shimadzu 330).

3. Result and discussion

3.1. Structural properties

The X-ray diffraction patterns of pure and doped films annealed in air at various temperatures are shown in Figure 1. As-grown n-YZO films exhibited an amorphous nature, whereas annealing at $350\ ^\circ\text{C}$ caused the conversion from the amorphous to the polycrystalline structure with (100), (002), and (101) peaks. It was observed that with an increase in annealing temperature from 350 to $450\ ^\circ\text{C}$, the (002) reflection peak became more intense and sharper as compared to the other peaks, indicating a preferential c -axis orientation.

Figure 2 shows the variation of the full-width half-maximum (FWHM) of the (002) peak with annealing temperature. The decrease of FWHM with increasing annealing temperature indicates an improvement in the crystallinity of the ZnO layer. No further improvement in crystallinity was observed at annealing temperatures above $450\ ^\circ\text{C}$ (up to $600\ ^\circ\text{C}$).

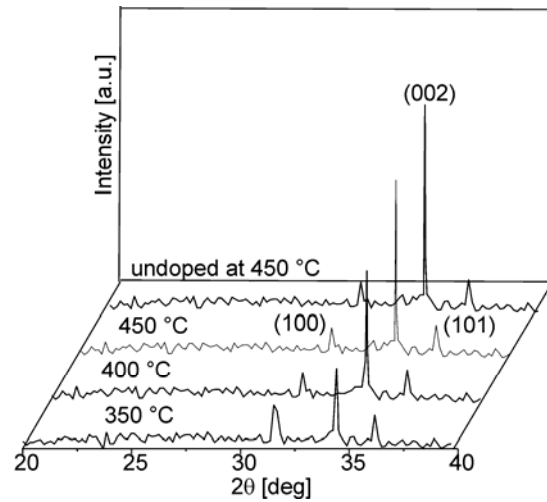


Fig. 1. XRD patterns of a YZO film on a Si substrate annealed at various temperatures

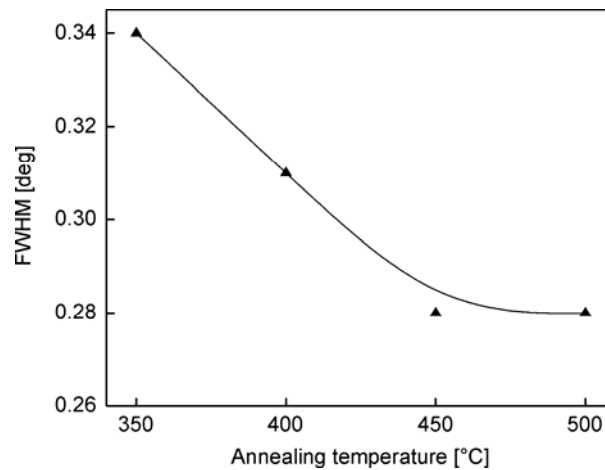


Fig. 2. Effect of annealing temperature on the FWHM of the (002) peak of a YZO film on a Si substrate

3.2. Optical transmittance

The transparency and homogeneity of pure and yttrium-doped ZnO thin films can be tested by optical transmittance measurements in the UV, VIS, and NIR ranges. The optical transmittance of pure and doped films on corning glass is shown in Figure 3. The films exhibit high transparency (>80%) in the visible region 400–800 nm. In the UV region, the optical transmittance falls sharply, indicating the onset of absorption in this region. The threshold of optical absorption shifts toward shorter wavelengths

for yttrium-doped ZnO films, suggesting an increase in the band gap due to yttrium doping. The observed optical interferences in the transmittance curve indicate a homogenous nature of the film.

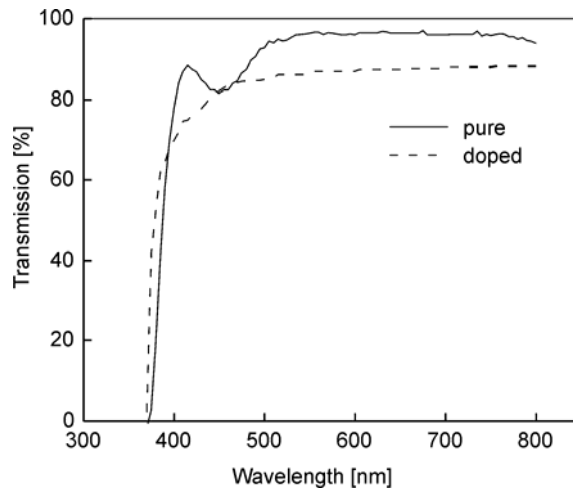


Fig. 3. Transmittance curves for pure and Y-doped ZnO films on corning glass annealed at 450 °C in air

3.3. Electrical properties

The electrical properties of the n-ZnO/p-Si heterostructures were investigated by I - U and C - U measurements. An attempt has been made to analyse the data theoretically. The I - U characteristics (I vs. U semi-logarithmic plots) of the heterojunction

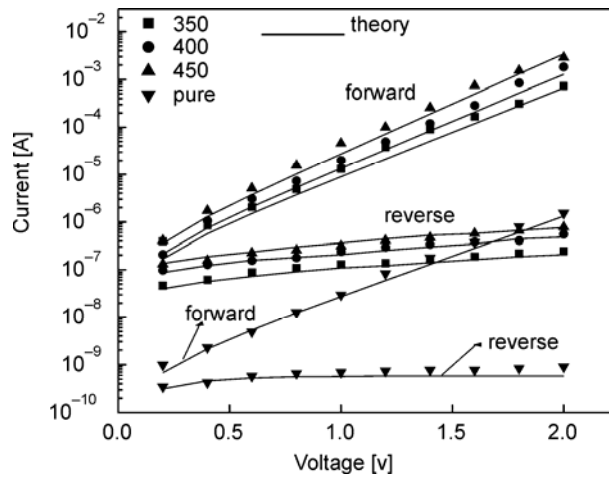


Fig. 4. Experimental and theoretical semi-logarithmic plots of I - U curves for the n-ZnO/p-Si heterostructure annealed at 350, 400, and 450 °C

n-ZnO/p-Si at various annealing temperatures are shown in Figure 4. A typical rectifying behaviour was observed for these heterostructures. With increasing annealing temperature, the current was found to increase both in the forward and reverse directions. The increase in the current can be caused by preferential *c*-axis growth of the n-ZnO films and/or a reduction of defect density at the interface with annealing temperature.

The energy profile of the heterojunction of the two semiconductors having different energy gaps is shown in Figure 5 in the equilibrium conditions. E_g , ε , χ , and ϕ represent the energy gaps, dielectric constants, electron affinities, and work functions of the two semiconductors, respectively. It can be seen from the figure that the discontinuity in the conduction band edges (ΔE_c) is equal to the difference in the electron affinities of the two semiconductors. The total built-in voltage (U_d) due to the difference in the work function ($\phi_1 - \phi_2$) is equal to the sum of built-in voltages on both sides.

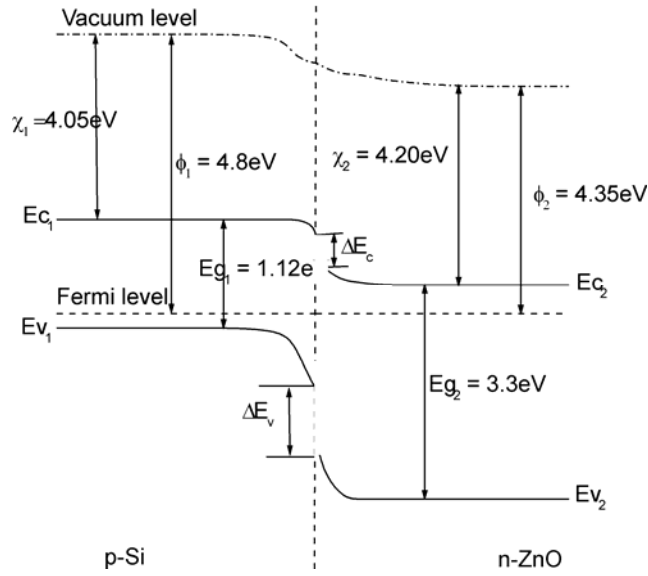


Fig. 5. Energy band profile of the n-ZnO/p-Si heterostructure

The current–voltage relation for the studied heterojunction, for which $\chi_1 < \chi_2 < \chi_1 + E_{g1}$ and $\phi_1 > \phi_2$, has been obtained by Perlman and Feucht [14] and is given below:

$$I = A \exp \left[\frac{-q(\Delta E_c + U_d)}{kT} \right] \times \left[\exp \left(\frac{qU}{kT} \right) - 1 \right] \quad (1)$$

where

$$A = aqXN_d \left(\frac{D_n}{\tau_n} \right)^{1/2}, \quad \Delta E_c = \chi_2 - \chi_1$$

U_d is the total built-in voltage, q is the electron charge, k is the Boltzman constant, T is temperature, a – the area of the diode, X – the transmission of electrons across the interface D_n if the diffusion constant, and τ_n is the lifetime of electrons in p-type materials. It may be mentioned that the experimental current values are much smaller than those predicted by this equation. The observed low values of current could be due to imperfections in the two semiconductors, resulting in defect states near the interface. Therefore, the current–voltage equation should be modified by introducing the imperfection parameter β ($\beta \geq 1$):

$$I = A \exp \left[\frac{-q(\Delta E_c + U_d)}{kT} \right] \times \left[\exp \left(\frac{qU}{\beta kT} \right) - 1 \right] \quad (2)$$

Using the above equation, the I – U characteristics were theoretically obtained. The values used for various parameters are given in Table 1. It was found that the value of β decreases from 9 to 8 as the annealing temperature increases from 350 to 450 °C for a unit area of the diode. The decrease in β suggests an improvement in heterostructure and reduction of defect state density at the interface with annealing. The defect density of states for the heterostructure annealed at the temperature of 450 °C was estimated by the C – U measurements.

Table 1. Physical parameters used to fit the electrical data of the n-ZnO/p-Si heterostructure

Annealing temperature [°C]	Donor concentration N_d [cm^{-3}]	β
450 (undoped)	2.4×10^{16}	10
350	5.1×10^{18}	9
400	5.95×10^{18}	8.5
450	9×10^{18}	8

To investigate the effect of annealing on the I – U characteristics, the values of N_d as obtained from Hall measurements were used in theoretical calculations. In the case of the undoped ZnO/Si heterostructure, the value of β was found to be 10, which is higher than that obtained for doped heterostructures.

The Mott–Schottky plot of a YZO/p-Si diode annealed at 450 °C and measured in the dark at room temperature is shown in Figure 6. The capacitance of the heterojunction is found to obey an approximately linear C^{-2} – U relationship in the reverse bias condition. This linear relationship implies that the depletion region in the vicinity of the heterojunction interface expands with increasing reverse bias. Since the band bending is primarily on the Si side, the C^{-2} – U intercept on the x -axis is essentially equal to the diffusion potential U_d within the Si. The slope of the line gives an estimate for defect density. At room temperature, the values of U_d and N were found to be 0.45 eV and $9.4 \times 10^{14} \text{ cm}^{-3}$, respectively. The data was analysed using the Anderson model.

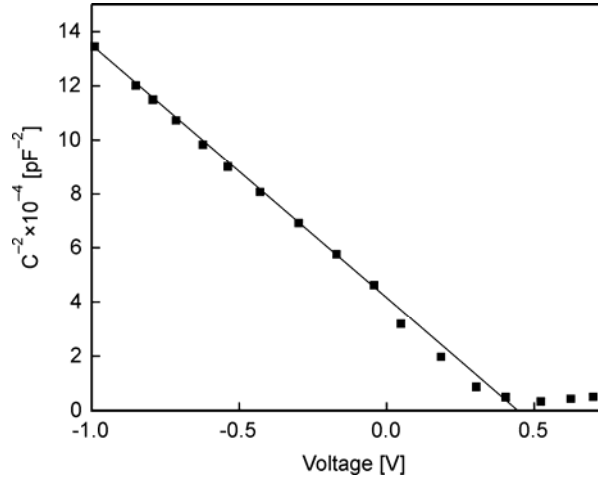


Fig. 6. C^{-2} - U curve for the n-ZnO/p-Si heterostructure at room temperature (300 K)

The C - U characteristics, as described by conventional heterojunction theory, can be expressed as

$$C^2 = \frac{q N \epsilon_1 \epsilon_2}{2} \frac{1}{(U_d - U_R)} \quad (3)$$

where U_R is the applied reverse voltage. Using this equation, we can estimate the effective density of defects from the slope of C^{-2} - U_R relationships. The value of $9.4 \times 10^{14} \text{ cm}^{-3}$ is obtained for $\epsilon_1 = 9$ and $\epsilon_2 = 11.9$, the electric permittivities of ZnO and Si, respectively. The potential barrier at the junction, as determined from the C^{-2} - U characteristics as the intercept on the x -axis, was found to be 0.45 eV. Anderson model [13] predicts that this is the energy difference of the work functions between Si and ZnO. The Fermi level below the vacuum level is 4.8 eV for p-Si and 4.35 eV for n-ZnO, as shown by the energy band profile of the heterojunction. These experimental results suggest that the junction between the n-ZnO thin film and p-Si substrate is governed by conventional heterojunction theory.

4. Conclusions

Yttrium-doped n-ZnO/p-Si heterostructures have been fabricated by depositing n-ZnO films on p-Si (100) using the sol-gel process. The I - U characteristics are found to improve with improving crystallinity of the ZnO films during annealing. The calculated height of the potential barrier at the junction, using C - U measurements, is found to be equal to the difference in the work function of ZnO and silicon. The imperfec-

tion parameter β , in the present case, is found to decrease with increasing annealing temperature. The defect density at the interface, as calculated from the Mott–Schottky plot at an annealing temperature of 450 °C, was found to be nearly 10^{15} cm^{-3} .

Acknowledgements

The authors wish to acknowledge the financial support of DRDO, Govt. of India, India.

References

- [1] XIONG G., WILKINSON J., TUZEMEN S., UCER K.B., WILLIAMS R.T., Proc. SPIE (2002), p. 4644.
- [2] SATO H., MINAMI T., TAKATA S., Thin Solid Films, 220 (1992), 327.
- [3] PETROU P., SINGH R., BRODIE D.E., Appl. Phys. Lett., 35 (1979), 930.
- [4] HU J., GORDON R.G., J. Appl. Phys., 71 (1992), 880.
- [5] NUNES P., MALIK A., FERNANDES B., FORTUNATO E., VILARINHO P., MARTINS R., Vacuum, 52 (1999), 45.
- [6] TANG W., CAMERON D.C., Thin Solid Films, 238 (1994), 83.
- [7] JEONG I.S., HOON K.J., SAONGIL I., Appl. Phys. Lett., 83 (2003), 2946.
- [8] LEE J.Y., CHOI Y.S., CHOI W.H., YEOM H.W., YOON Y.K., KIM J.H., SAONGIL I., Thin Solid Films, 420 (2002), 112.
- [9] PARK C.H., JEONG I.S., KIM J.H., SAONGIL I., Appl. Phys. Lett., 82 (2003), 3973.
- [10] PURICA M., BUDIANU E., RUSU E., Thin Solid Films, 383 (2001), 284.
- [11] BAIK D.G., CHO S.M., Thin Solid Films, 354 (1999), 227.
- [12] PERLMAN S.S., FEUCHT D.L., Solid State Electron., 7, (1964), 911.
- [13] ANDERSON R.L., Solid state Electron., 5 (1962), 283.
- [14] KAUR R., SINGH A.V., MEHRA. R.M., Mater. Sci.-Poland, 22 (2004), 201.

Received 23 September 2005

Revised 4 December 2005